Asian Journal of Chemistry; Vol. 26, No. 17 (2014), 5329-5332

ASIAN JOURNAL OF CHEMISTRY

http://dx.doi.org/10.14233/ajchem.2014.18103

Mechanical Behaviour of Titanium Oxide-Coated Vessel Stents†

Zhonghua Min[1], Nan Huang[2], Hengquan Liu[1,3,*] and Qinyong Zhang[1]

[1]Center for Advanced Materials & Energy, Xihua University, Jinniu District, Chengdu 610039, Sichuan Province, P.R. China
[2]School of Material Science & Technology, Southwest Jiaotong University, Chengdu 611756, P.R. China
[3]Department of Research & Development, Kinhely Bio-Tech Co., Ltd., P.R. China

*Corresponding author: Fax: +86 755 83073251; Tel: +86 755 83073249; E-mail: liuhengquan@kinhely.com

AJC-15692

Vascular vessel stents were coated with titanium oxide (Ti-O) by a physical vapor deposition method. The composition, coating thickness and mechanical behaviour of the coating were investigated during stent compression and dilatation. The surface area and thickness of the Ti-O coating were calculated using known parameters. The composition of the coating was characterized *via* energy dispersive X-ray spectroscopy. The mechanical behaviour of the coating was investigated during stent deformation, particularly in regions experiencing high stress during compression or expansion. Results show that the Ti-O coating is smooth and uniform. There were no cracks or delaminations on the stent surface after dilation by angioplasty, indicating sufficient adhesion of the Ti-O coating to the stent.

Keywords: Vessel stent, Ti-O Coating, Deformation, Mechanical behaviour.

INTRODUCTION

Stent implantation procedures aim to prevent or manage angioplasty-associated complications, including stenotic vessel recoil and vessel dissection, with the ultimate goal of preventing early restenosis[1,2]. Stent implantation avoids over distension of the vessel and therefore markedly reduces the risk of aneurysm formation or vascular wall dissection compared to angioplasty procedures[3]. However, in-stent stenosis has become a new clinical problem for metallic stents[4]. Recent work evaluating the biocompatibility of metallic stents has demonstrated that metal ions released from corroded stents are potentially toxic and cause endothelial cell damage. The metal ions also increase the thrombogenicity of the stents by inducing platelet activation[5-7]. To address these issues, a potential approach is to develop a stent coating using a material that can reduce excessive corrosion while remaining biocompatible[8]. For example, stents with bioceramic coatings are an attractive solution because they offer both desired mechanical properties and desired chemical stability due to their metallic components and ceramic coatings, respectively[9]. Recent work over the past decade has also highlighted the excellent antithrombotic properties of titanium oxide (Ti-O)[10,11], suggesting that Ti-O coatings may have great potential to address current problems with stent biocompatibility and corrosion[11,12]. In order to develop Ti-O-coated stents for implantation *in vivo*, the adhesion strength and uniformity of the coating must be optimized to maximize stent longevity.

Our experiments have shown that a biocompatible Ti-O coating was achieved by metal vacuum arc source magnetron sputtering, thus demonstrating the feasibility of fabricating Ti-O coatings on vessel stents using this technology. In this work, metal vacuum arc source deposition was used to fabricate Ti-O coatings of various thicknesses on L-605 stents. The composition and thicknesses of the Ti-O coatings were characterized using traditional analysis methods and the mechanical behaviour of the coated stents was evaluated by simulation of *in vivo* stent operation.

EXPERIMENTAL

Ti-O film was deposited on vessel stents *via* metal vacuum arc source deposition, the optimal parameters of preparation referenced prior works[13] . Bare and Ti-O-coated stents were expanded by PTA balloon dilation and their mechanical properties were investigated after compression or expansion. Mechanical behaviour of the coating was analyzed by observing the maximum deformed cell of the compressed or expanded stent. Scanning electron microscopy (SEM) was employed to observe coating adhesion strength after deformation. At least six stents were tested on the different parts of each sample (n = 3).

†Presented at 2014 Global Conference on Polymer and Composite Materials (PCM2014) held on 27-29 May 2014, Ningbo, P.R. China

General procedure: The substrate surface was cleaned by argon ion for 10 min at a working pressure of about 0.60 Pa and a sputtering bias of 32V. The stents were mounted on a rotating substrate holder, with a distance of about 25 mm between the stents and cathodic arc targets. During Ti-O deposition, oxygen was introduced into the vacuum chamber at a partial pressure of 0.2 Pa. Further parameters for the deposition procedure are presented in Table-1.

Detection method: The morphology of the Ti-O coating was characterized using motic microscopy (Motic group-plus 2.0 mL). The coating composition was characterized by energy dispersive X-ray spectroscopy (EDX, 6510A, Shimadzu). Chemical states of elements of the films were analyzed using X-ray photoelectron spectrometer with an MgKα (hv = 1253.6 eV) line excitation source. The binding energy scale was referenced by setting the Cls peak to 284.6 eV.

The surface area of the stent was calculated using known values for the weight and density of the stent and the thickness of coating was calculated using known values for the surface area and the weight of the coating, as described below.

The basic unit of the stent is composed of support unit and bridge cell. Therefore, this structure may be represented as a schematic of simplified stent cell unit (Fig. 1). The following formulae for the surface area and volume of the stent cell are therefore obtained:

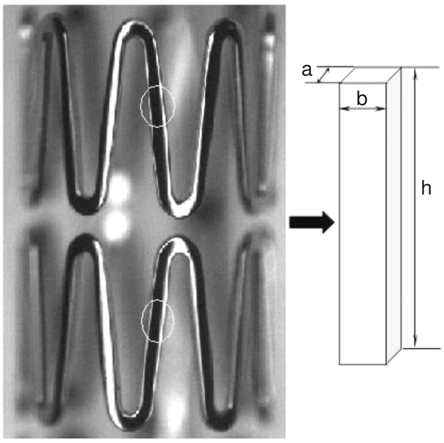

Fig. 1. Sketch chart using to calculate acreage of stent

$$S = 2(a + b)h \quad (1)$$

$$V = \frac{m}{t} = abh \quad (2)$$

where a, b and h are the length, width and height of the cell unit, respectively; and V, S, m and t are the volume, surface area, weight and density, respectively, of the cell unit.

Formula 3 is obtained by substituting formula 2 into formula 1:

$$S1 = \frac{2m(a + b)}{abt} \quad (3)$$

Assuming a uniform Ti-O coating on the inner and outer surfaces of the cell unit, the thickness (T) of the coating can be derived (formula 4):

$$T = \frac{M - m}{\rho S_1} \quad (4)$$

where ρ, M and m are the density of Ti-O, the weight of the Ti-O-coated stent and the weight of the bare stent, respectively.

In order to compare above model, the surface profilometry (AMBIOS XP-2) was employed to determine actual thickness, which value is obtained from Ti-O film modified plate instead of vessel stent, but the Ti-O film of both sample is identical via same fabrication parameter.

RESULTS AND DISCUSSION

Motic microscopy images of both bare and modified stents are shown in Fig. 2. The coated stent has a smoother surface that does not exhibit any macro-particles on the surface of the Ti-O coating. Surface composition of the Ti-O-coated stent was also studied by EDX. The EDX spectra shown in Fig. 3 verify that Ti and O atoms are present on the modified stent. Stent surfaces also had high cobalt and chromium concentrations. Oxygen and titanium concentrations on the outer surface of the stent are relatively higher than on the inner surface, indicating that more Ti-O particles were deposited on the outer surface compared to the inner surface. Fig. 4 shows the high-resolution XPS spectra of the Ti2p peaks of the Ti-O film after being etched by Ar^+ for 1 min. The XPS of Ti2p spectrum was fitted with one peak at the binding energy of 285.1 eV, as the Ti present primarily existed in the TiO state. It must be noted that some absorbed or residual molecular oxygen may be present in the vacuum in the XPS chamber and oxidation may have already occurred on the sputtered titanium film.

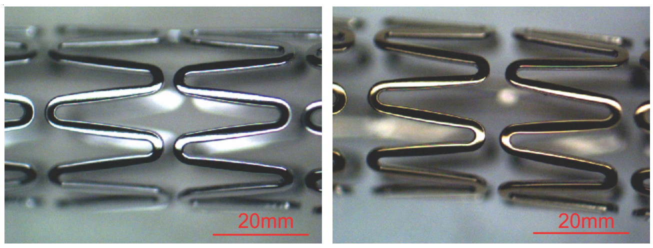

Fig. 2. Motic images showing the morphology of the surface of stents (a) is surface of bare stent and (b) is modified ones separately

The thickness of the Ti-O coating was calculated to be 15 nm *via* modeling. But the thicknesses of stent surface is about 20 nm by profile curve, this value is thought to represent the actual thickness of a Ti-O-coated stent when treated under the same conditions (Fig. 5). SEM images of the Ti-O-coated stents are shown in Fig. 6. The Ti-O coating on the stent surface is smooth and uniform and there are no visible cracks or particles

TABLE-1
PARAMETERS FOR Ti-O DEPOSITION

Flow rate (Ar) (sccm)	Sputtering power (W)	Flow rate(O_2) (sccm)	Sputtering bias-votage (V)	Sputtering current (A)	Particle beam (mA)	Deposited time (min)
95	160	50	30	$I_1 = 1.4, I_2 = 5, I_3 = 0$	160-200	5

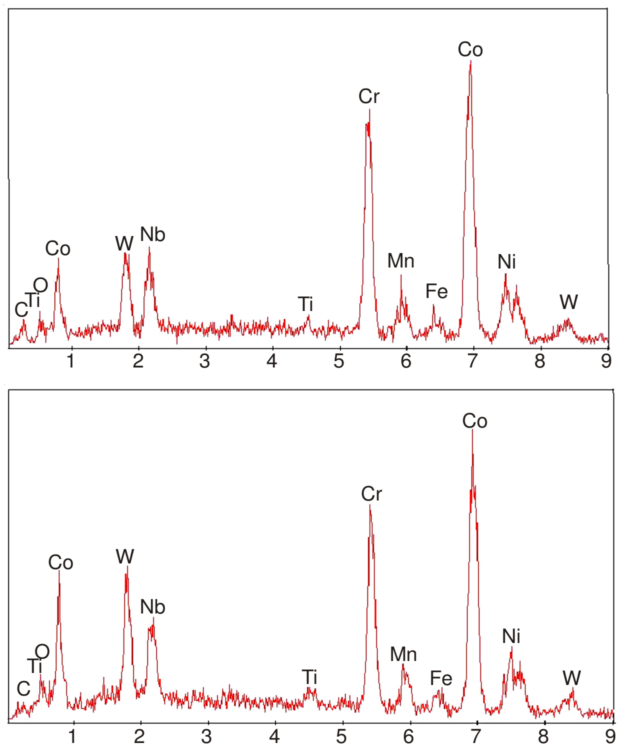

Fig. 3. EDX spectrum of modified stents, a is outer side of stent struts, b is inner side of stent struts, respectively

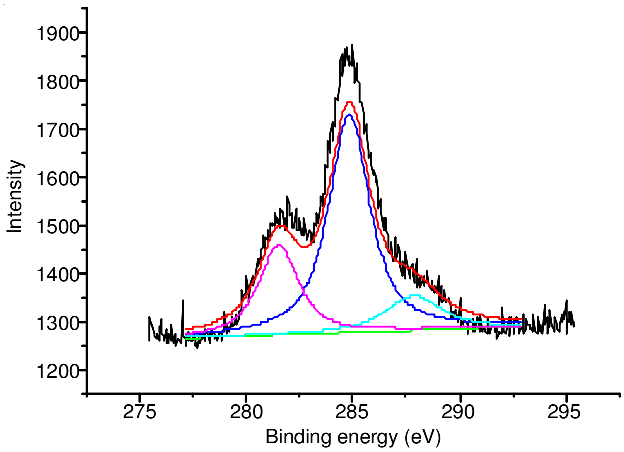

Fig. 4. High-resolution XPS spectra of Ti2p peaks

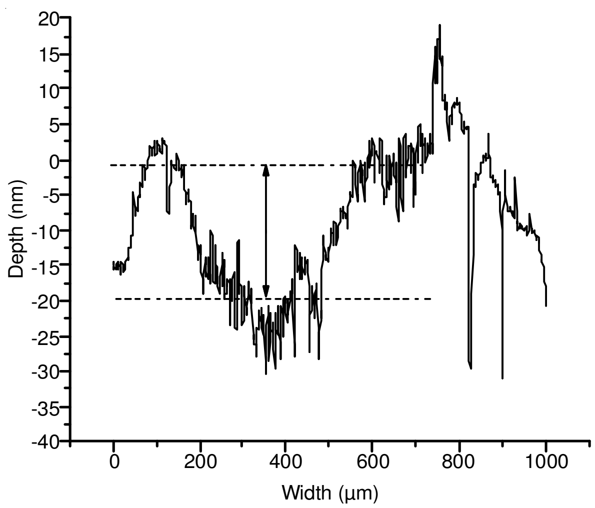

Fig. 5. Profile curve of Ti-O film modified pieces

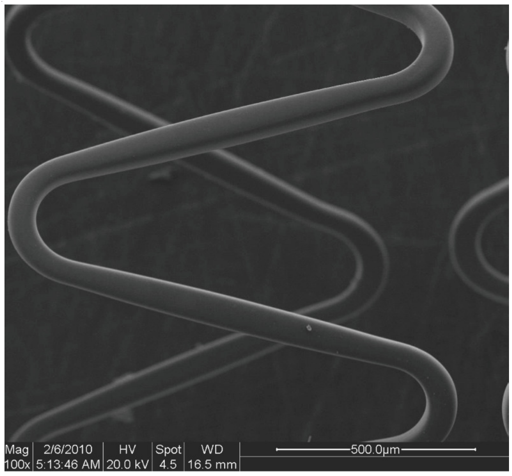

Fig. 6. SEM image showing the morphology of a Ti-O-coated stent

on the stent surface. During the Ti-O coating process, it is possible for Ti-O atoms to be deposited non-uniformly on the stent surface. Such a surface defect would result in compactability and inner stress, factors that influence the adhesion strength between the coating and the metal substrate[14]. Clinical studies have demonstrated that uniformity, delamination and damage of stent coatings are directly correlated to patient safety. The mechanical behaviour of Ti-O coatings after stent deformation may be evaluated *in vitro* to model their performance *in vivo*. SEM images of the deformed stent cell are shown in Fig. 7. These images show that the Ti-O coating is still smooth and uniform after dilation. The deformed stent cell does not exhibit any cracks, delaminations or damage.

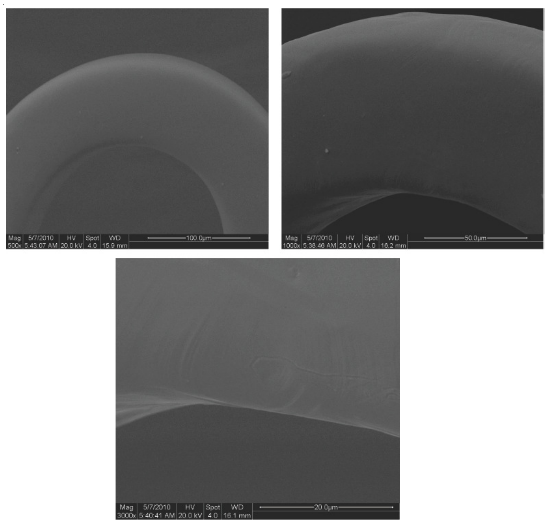

Fig. 7. SEM images of a deformed stent cell under different magnification powers

In order to evaluate the mechanical properties of the coating at regions of concentrated mechanical stress, the most deformed cell was selected to observe under three different magnification power levels (500x, 1000x and 3000x). Although several slip lines were seen at 3000x magnification power, neither delamination nor damage of the coating were observed, indicating that the Ti-O coating can adhere tightly to the stent surface. The adhesion between a coating and its substrate should be strong to ensure extended stent longevity *in vivo*[15].

In addition, the coating should be uniform and should cover the stent surface completely. Ti-O coated stents can be prepared by methods such as ion beam-assisted deposition or chemical vapor deposition. However, it is difficult and expensive to deposit a uniform layer of Ti-O on stents with complex shapes or geometries using these methods[16]. Metal vacuum arc source deposition, however, can achieve uniform coatings on complex stent geometries. Furthermore, the Ti-O coatings generated by this technique can withstand the compressive and expansion stresses experienced during stent mounting and deployment.

Conclusion

This work reports successful deposition of a Ti-O coating on L-605 coronary stents by metal vacuum arc source deposition. The surface of all coated stent cells was observed to be smooth and uniform and the thickness of the Ti-O coating was about 15 nm. There were no cracks or delaminations on the stent surface after dilation by angioplasty, indicating sufficient adhesion of the Ti-O coating to the stent.

ACKNOWLEDGEMENTS

This work was jointly and financially supported by Key Basic Research Project No. 2005CB623904, NSFC (20603027).

REFERENCES

1. I.K. Stefanids, V.A. Tolis, D.G. Sionis and L.K. Michalis, *Hellenic J. Cardiol.*, **43**, 63 (2002).
2. A. Schomig, A. Dibra, S.A. Windecker, J. Mehilli, J. Suárez de Lezo, C. Kaiser, S.-J. Park, J.-J. Goy, J.-H. Lee, E. Di Lorenzo, J. Wu, P. Jüni, M.E. Pfisterer, B. Meier and A. Kastrati, *J. Am. Coll. Cardiol.*, **50**, 1373 (2007).
3. J.E. Sousa, M.A. Costa, A.G.M.R. Sousa, A.C. Abizaid, A.C. Seixas, A.S. Abizaid, F. Feres, L.A. Mattos, R. Falotico, J. Jaeger, J.J. Popma and P.W. Serruys, *Circulation*, **107**, 381 (2003).
4. J.M. Garasic, E.R. Edelman, J.C. Squire, P. Seifert, M.S. Williams and C. Rogers, *Circulation*, **101**, 812 (2000).
5. A. Dibra, A. Kastrati, J. Mehilli, J. Pache, H. Schühlen, N. von Beckerath, K. Ulm, R. Wessely, J. Dirschinger and A. Schömig, *N. Engl. J. Med.*, **353**, 663 (2005).
6. I. Tsyganov, M.F. Maitz and E. Wieser, *Appl. Surf. Sci.*, **235**, 156 (2004).
7. S.N. David Chua, B.J. MacDonald and M.S.J. Hashmi, *Mater. Process. Technol.*, **155-156**, 1772 (2004).
8. T. Hanawa, *Mater. Sci. Eng. C*, **24**, 745 (2004).
9. F. Zhang, Z.H. Zheng, Y. Chen, X. Liu, A. Chen and Z. Jiang, *Biomed. Mater. Res.*, **42**, 128 (1998).
10. W. Walke, Z. Paszenda and J. Filipiak, *J. Mater. Process. Technol.*, **164-165**, 1263 (2005).
11. N. Huang, P. Yang, Y.X. Leng, J.Y. Chen, H. Sun, J. Wang, G.J. Wang, P.D. Ding, T.F. Xi and Y. Leng, *Biomaterials*, **24**, 2177 (2003).
12. M. Pourbaix, L. Klimzack-Mathieiu, C. Mertens, J. Meunier, C. Vanleugenhaghe, L. de Munck, J. Laureys, L. Neelemans and M. Warzee, *Corros. Sci.*, **3**, 239 (1963).
13. H. Liu, Y. Leng and N. Huang, *J. Mater. Eng. Perform.*, **21**, 424 (2012).
14. D.M. Mattox, *Surf. Coat. Technol.*, **81**, 8 (1996).
15. Y.X. Leng, J.Y. Chen, P. Yang, H. Sun, J. Wang and N. Huang, *Nuclear Instrum. Methods Phys. Res. Sec. B*, **242**, 30 (2006).
16. I. Menown, R. Lowe and I. Penn, *J. Invasive Cardiol.*, **17**, 222 (2005).